




Development of the simple analytical method for determination of arsenate(V) ion using fluorescence-labeled DNA and cerium oxide nanoparticles

Koji Matsunaga ^{a,*}, Hisashi Satoh ^a and Reiko Hirano ^b

^a Division of Environmental Engineering, Faculty of Engineering, Hokkaido University, North-13, West-8, Sapporo 060-8628, Japan

^b Cellspect Co., Ltd, 1-10-82 Kitaiioka, Morioka, Iwate 020-0857, Japan

*Corresponding author. E-mail: k-matsunaga_7dnd@eis.hokudai.ac.jp

 KM, 0000-0002-4652-3427; HS, 0000-0002-5222-9689; RH, 0000-0002-2022-2482

ABSTRACT

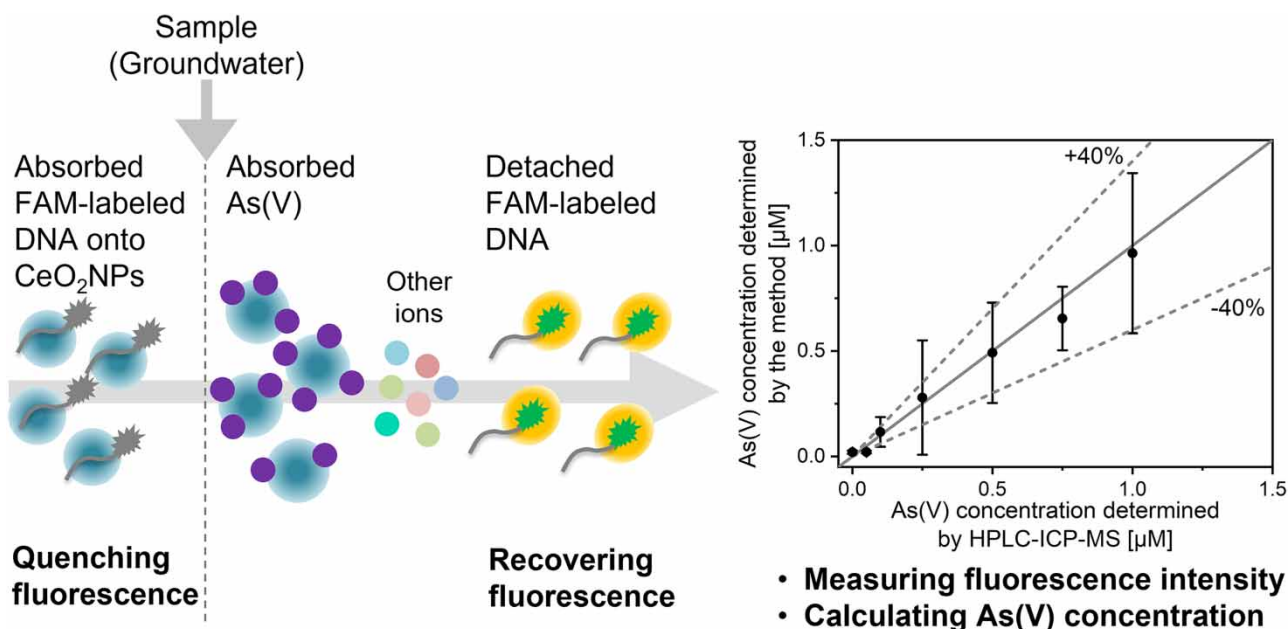
Arsenic (As) contamination in groundwater presents a major health and environmental concern. As is found in two oxidation states and most chemical tests for inorganic arsenic are focused on As(III), and few have been developed for As(V). We developed the simple analytical method for determining As(V) concentrations in groundwater using CeO₂NPs and fluorescein (FAM)-labeled DNA. Prior to sample measurements, we investigated the key operational parameters that affect the sensing performance. The optimal CeO₂NPs final concentration, FAM-labeled DNA final concentration, the sequence and length of FAM-labeled DNA, and incubation time were 15 µg/mL, 400 nM, 6-mer polycytosine sequence, and 6 min, respectively. After optimizing the parameters, the total analysis time was about 20 min and the limit of detection was 0.61 µM. This method has a high selectivity against the same concentrations of Cu(II), Cd(II), Hg(II) and Pb(II). Pretreatment by cation extraction to remove interfering ions was beneficial for determination of As(V) concentrations in groundwater containing a variety of metal cations at high concentration. We could determine As(V) concentration in groundwater. Modification of the reactions of the method is necessary. This study provides the first step in the development of a simple method for on-site As(V) analysis.

Key words: arsenate, groundwater, nanoparticles, simple analytical method, single-stranded DNA

HIGHLIGHTS

- Cerium oxide nanoparticles-based fluorescence method for As(V) determination was developed.
- Parameters that influence the method were optimized.
- Most groundwaters could determine As(V) concentrations roughly.

GRAPHICAL ABSTRACT



INTRODUCTION

Inorganic arsenic (As) is extremely toxic, leading to a serious threat including cardiovascular, respiratory diseases, and cancers of skin, lung, liver and kidney (Chung *et al.* 2013; Flora 2015; Singh *et al.* 2015). Its contamination of drinking water sources was estimated to affect human health over 144 million people around the world (Clancy *et al.* 2013). Because of the high toxicity of As, the World Health Organization (WHO) and the US Environmental Protection Agency (USEPA) set the primary maximum contaminant level (MCL) for total As in drinking water as low as 10 µg/L (WHO 2011; USEPA 2018). Chowdhury *et al.* (2000) reported that more than 100 µg/L-As concentrations have been detected in about 47.9% of well water and the lower As concentrations are less than 10 µg/L and the upper As concentrations are higher than 1000 µg/L in Bangladesh. Amini *et al.* (2008) modeled probability maps of global As contamination using a large database of measured As concentration in groundwaters from around the world and digital maps of physical characteristics such as soil, geology, climate and elevation. They showed that most countries could have contamination of As higher than 10 µg/L (Amini *et al.* 2008).

Some commercial instruments which are commonly used for As determination include atomic absorption spectrometry (AAS), atomic fluorescence spectrometry and inductively coupled plasma mass spectrometry (ICP-MS), hydride generation atomic absorption spectrometry (HG-AAS), electrothermal atomic absorption spectrometry (ETAAS), flow injection-hydride generation-inductively coupled plasma mass spectrometry (FI-HG-ICPMS), anodic stripping voltammetry (ASV), and cathodic stripping voltammetry (CSV) using a hanging drop mercury electrode (Das & Sarkar 2016). Although these traditional techniques have excellent accuracy and sensitivity, they require sophisticated, expensive and bulky equipment, specialized expertise for operation, and high operating cost. Hence, they are not suitable for on-site analysis (Wu *et al.* 2012a; Kaur *et al.* 2015).

Inorganic As has two common oxidation states: arsenate (As(V)) and arsenite (As(III)). Most chemical and biological sensors have been developed to determine As(III) (Baghbaderani & Noorbakhsh 2019) or total As based on using DNA aptamer (Wu *et al.* 2012b; Zhan *et al.* 2014; Matsunaga *et al.* 2019) or the redox properties and strong thiophilicity of As (Pena-Pereira *et al.* 2018; Xu *et al.* 2019). However, those assays could not determine As(V) alone although some commercial kits are available for As detection. They rely on the reduction of As(III) species in solution by zinc to form arsine gas (Lopez *et al.* 2017). While it is more challenging to detect As(V) alone, a few studies to detect As(V) have also been developed, which use polymer hydrogels, small molecules, gold nanoparticles, and bimetallic NPs (Lopez *et al.* 2017).

Recently, there has been interest in using nanomaterials for analytical applications. The nanomaterials in general have a high specific surface area and may offer high sensitivity. One of the nanomaterials is metal oxide nanoparticles (MONPs).

The MONPs were carried out for their ability to adsorb DNA, quench fluorescence (Pautler *et al.* 2013), and release DNA in the presence of target anions (Liu & Liu 2015). DNA-functionalized MONPs may be useful as a sensor platform for anion detection. In previous studies, iron oxide nanoparticles ($\text{Fe}_3\text{O}_4\text{NPs}$) are used as the As(V) sensor because As(V) binds to $\text{Fe}_3\text{O}_4\text{NPs}$ surface (Liu & Liu 2014, 2015). Another study showed that cerium oxide nanoparticles (CeO_2NPs) was a general oxidase that could oxidize many substrates (Pautler *et al.* 2013). CeO_2NP also adsorbed As(V) on its surface and its DNA adsorption affinity was stronger than that of $\text{Fe}_3\text{O}_4\text{NP}$ (Liu & Liu 2015; Lopez *et al.* 2017; Bülbül *et al.* 2018). However, their application for environmental monitoring has been extremely limited because of the lack of selectivity (Lopez *et al.* 2017; Muppudathi *et al.* 2019). Here, we developed a simple analytical method for determination of As(V) concentrations in various kinds of groundwater by fluorescence spectroscopy.

MATERIALS AND METHODS

Principle of our method

Figure 1 shows the sensing mechanism of the method. First, fluorescein (FAM)-labeled DNA is incubated with CeO_2NPs . FAM-labeled DNA is adsorbed onto the CeO_2NP surface and the fluorescence may be quenched. Second, samples are added into the solution. In the absence of As(V), FAM-labeled DNA- CeO_2NPs complex remains in the solution. In contrast, As(V) displaces the adsorbed FAM-labeled DNA from the CeO_2NPs , resulting in recovery of fluorescence signal. Therefore, a quantitative analysis of the As(V) concentration is possible by measuring the fluorescence intensity derived from FAM (Ex: 495 nm, Em: 520 nm).

Chemicals and materials

All of the FAM-labeled DNA were from Eurofins Genomics K.K. (Tokyo, Japan). Table 1 shows the list of sequences which were used in this study. 4-(2-hydroxyethyl)-1-piperazineethanesulfonic acid (HEPES) was from Nakalai tesque, INC. (Kyoto, Japan). CeO_2NPs as a 10 wt.% in H_2O (catalogue number 643009-100ML) was from Sigma-Aldrich Japan (Tokyo, Japan). As(V) as a 60% arsenic acid solution (H_3AsO_4 , catalog number 013-04675) was from Fujifilm Wako Pure Chemical Corporation (Osaka, Japan). All solutions were prepared with Milli-Q Water (Merck Millipore, Tokyo, Japan).

Determination of As(V) using CeO_2NPs and FAM-labeled ssDNA

The probe solution was prepared by adding CeO_2NPs dispersion and FAM-labeled DNA solution to the 10-mM HEPES buffer solution (pH: 7.6). After 15 minutes, a 20- μL probe solution was added into the microtubes. A 20- μL sample solution

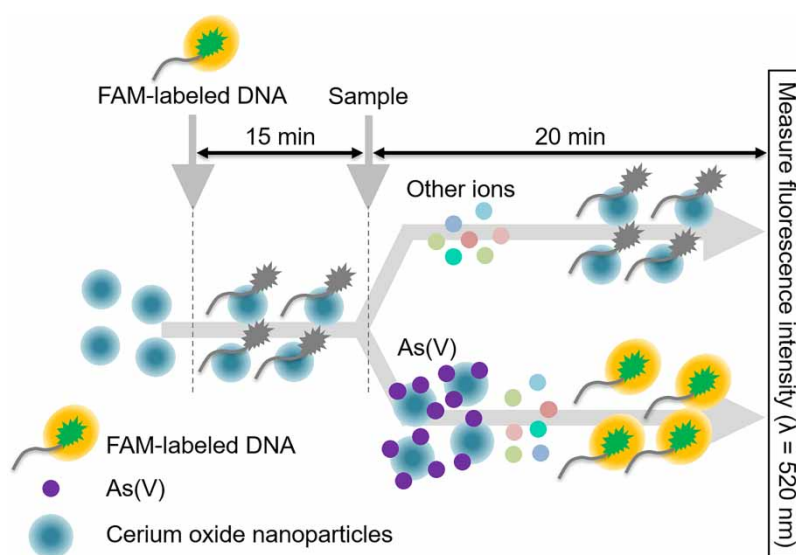


Figure 1 | Schematic representation of the colorimetric detection of As(V) in aqueous solution based on an FAM-labeled ssDNA and cerium oxide nanoparticles.

Table 1 | DNA sequences used in this study

DNA Name	Sequences
FAM-C ₆	5'-[FAM]-CCCCCC-3'
FAM-C ₁₂	5'-[FAM]-CCCCCCCCCCCC-3'
FAM-C ₁₈	5'-[FAM]-CCCCCCCCCCCCCCCCCCCC-3'
FAM-C ₂₄	5'-[FAM]-CCCCCCCCCCCCCCCCCCCCCCCCCCCC-3'
FAM-C ₃₀	5'-[FAM]-CCCCCCCCCCCCCCCCCCCCCCCCCCCCCCCCCCCC-3'

was mixed with the probe solution in the microtube. After incubation of the mixture at room temperature for 20 min, the fluorescence intensity at 518 nm in the test solution was measured.

We examined the effects of the concentrations of CeO₂NPs and FAM-labeled ssDNA, the length of FAM-labeled ssDNA and the incubation time with samples on the method sensitivity. To optimize the concentration of CeO₂NPs and FAM-labeled ssDNA, the final CeO₂NPs concentrations of the test solutions were changed from 0 to 60 µg/mL and the final FAM-labeled ssDNA concentrations were changed from 0 to 500 nM after the optimization of final CeO₂NPs concentration. We compared the fluorescence intensity at 518 nm of the sample with 1-µM As(V) (POS) and one without As(V) (NEG). To optimize the length of the DNA, FAM-labeled poly-cytosine DNAs (Table 1) were used to study As(V)-induced DNA detachment reaction. All of the data were used to calculate ΔF, which is the difference between the fluorescence intensity of the POS and the NEG samples. To optimize the incubation time after adding the samples, three test solutions of the POS and the NEG samples, respectively, were incubated for 30 min after adding the sample, and the fluorescence intensities were measured every 6 min and ΔF was calculated.

After optimization of the parameters described above, we created a calibration curve of the method at a variety of As(V) concentrations. The fluorescence spectra of 10 blank samples (using Milli-Q water as the samples) and three samples of As(V) standard solution at individual As(V) concentrations were measured. The fluorescence peaks at 518 nm were plotted against the corresponding As(V) concentrations. A linear regression was also used to obtain a calibration curve at As(V) concentrations above 0.5 µM. Based on the results, the limit of detection (LOD) value was estimated using an equation, $3\sigma/s$, where σ is the standard deviation of 10 blank samples and s is a slope of the regression line.

Selectivity of the method was assessed by measuring the fluorescence intensities of the test solutions with H₃AsO₄, NaAsO₂, H₃BO₃, NaHCO₃, Na₂CO₃, NaNO₃, NaF, K₂HPO₄, Na₂SO₃, Na₂SO₄, Na₂SeO₄, KBr and KI at 10 µM, which were against As(V) for the environmentally important anions. For the cations, we used NaCl, MgCl₂·6H₂O, KCl, CaCl₂, MnCl₂·4H₂O, FeCl₂·4H₂O, FeCl₃·6H₂O, CoCl₂, NiCl₂·6H₂O, CuCl₂·2H₂O, ZnCl₂, HgCl₂ and (CHCOO)₂Pb·3H₂O as the selectivity test. ΔF were compared among these samples by Steel test.

Groundwater samples (GW) were taken in February 2019. Since the GW did not contain As, As(V) was spiked to the GW at different concentrations for determination tests. The samples were filtered through a 0.2-µm pore-size membrane (Advantec Co., Ltd, Japan) and then passed through a cation-exchange column (MetaSEP IC-MC, GL Sciences, Tokyo, Japan). Thereafter, As(V) concentrations were determined using our method and ICP-MS and HPLC-ICP-MS and both were compared.

Instrumentation and software

The fluorescence intensity was measured by using a fluorescence spectrophotometer FP-6600 (JASCO Corporation, Tokyo, Japan). The metal-ion concentrations in groundwater were measured by ICP-MS 8800 ICP-QQQ (Agilent, United States) and HPLC-ICP-MS system, which were passed through a GelPack GL-IC-A column (Hitachi Chemical) connected to a high performance liquid chromatograph (Shimadzu, SLC-10Avp system), and introduced to an inductively coupled plasma mass spectrometer (ICP-MS, Thermo, iCAP Qc) (Kamei-Ishikawa *et al.* 2017). R version 3.5.2 was used for the statistical analysis in this study.

RESULTS AND DISCUSSION

Effect of CeO₂NPs and FAM-labeled DNA concentrations on fluorescence intensity

Because the CeO₂NPs and FAM-labeled ssDNA concentrations are the most important of all parameters, the effect of final CeO₂NPs concentration and FAM-labeled DNA concentration on the fluorescence intensity were investigated. Figure 2 shows the effect of the final CeO₂NPs concentrations on fluorescence intensity of the POS and NEG samples. The

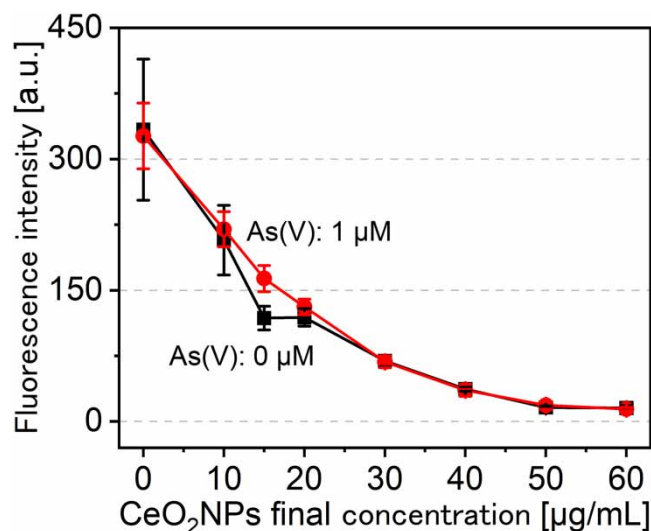


Figure 2 | Effect of the final CeO₂NPs concentrations of the test solutions on fluorescence intensity in the presence (POS) and absence of As(V) (NEG). FAM-C₆ as FAM-labeled ssDNA was used. The final FAM-C₆ concentration was 375 nM. The incubation time after sample addition was 20 min.

fluorescence intensity decreased as the concentration of CeO₂NPs increased in both samples. Only at 15 µg/mL of CeO₂NP concentrations, the fluorescence intensity of the POS sample became higher than the NEG sample and there was a statistically significant difference ($p=0.05$). Because the difference in fluorescence intensity of the POS and NEG samples is related to the sensitivity of the method, the final CeO₂NPs concentration of a test solution was determined to be 15 µg/mL.

At 0–10 µg/mL, there was no difference between POS and NEG due to the low amount of As(V) detached. At 20 µg/mL or higher, the amount of CeO₂NPs was higher than that of FAM-C₆ in the test solution. We thought it was because the pentavalent As adsorbed on the free CeO₂NPs and was not desorbed by adding FAM-C₆.

We performed the adsorption equilibrium experiments to calculate the detachment constant (K_d) of the FAM-labeled ssDNA from CeO₂NPs. In the adsorption equilibrium experiments, 20-µL aliquots of the probe solution were added into 1.5-mL tubes. The probe solution was prepared by adding CeO₂NPs dispersion (0–60 µg/mL) and FAM-labeled ssDNA solution (400 nM) to the 10-mM HEPES buffer solution (pH: 7.6). 10-mM HEPES buffer solution (pH: 7.6) was prepared as a control sample. After measuring the fluorescence intensity, we calculated the concentration of adsorbed ssDNA using the calibration curve of the fluorescence intensity at 518 nm versus the concentration of FAM-labeled DNA. The obtained data were fitted to the Langmuir models using Equation (1) (Hafuka *et al.* 2019);

$$q_e = Q_b C_e / (1 + b C_e) \quad (1)$$

where q_e is the concentration of ssDNA that adsorbed onto CeO₂NPs (nM), C_e is the equilibrium concentration of non-adsorbed ssDNA (nM), Q_m is the maximum adsorption capacity of ssDNA (nM) and b is the constant related to the energy of adsorption. As a result, the binding curve was fitted to the plots of the NEG samples and the K_d of DNA from CeO₂NPs was calculated to be 5.17 µg/mL (Figure S1).

We also optimized the final FAM-labeled ssDNA concentration (Figure 3). The difference of fluorescence intensity of the POS and NEG samples increased as the final concentration of FAM-labeled DNA was increased. The ΔF were the highest (75.2) at 400 nM of FAM-labeled ssDNA. It decreased when the FAM-labeled ssDNA concentration was 500 nM, but we considered that it was a measurement error because there was no statistically significant difference ($p=0.05$) between the results at 400 and 500 nM. Based on these results, the final concentration of FAM-labeled DNA was determined to be 400 nM.

Effect of the length of FAM-labeled DNA on fluorescence intensity

It was expected that the ssDNA length would affect the As(V)-induced ssDNA detachment reaction (Liu & Liu 2014). Therefore, we investigated the effect of ssDNA length on ΔF . We used FAM-C_n (n changes from 6 to 30) (Figure 4). The previous

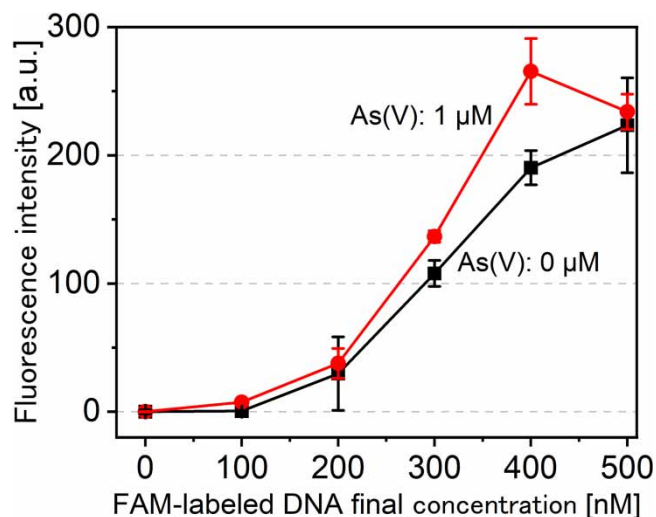


Figure 3 | Effect of final FAM-labeled DNA concentration of test solutions on fluorescence intensity in the POS and NEG. The final CeO_2NPs concentration was $15\ \mu\text{g/mL}$, FAM- C_6 as FAM-labeled DNA was used and the incubation time after sample addition was 20 min.

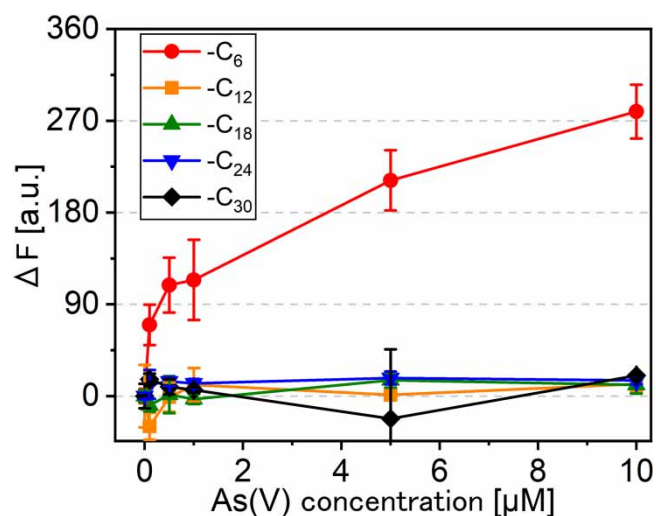


Figure 4 | Effect of DNA length on calibration curves. The final CeO_2NPs concentration was $15\ \mu\text{g/mL}$, the final concentration of each FAM-labeled DNA was 400 nM and the incubation time after sample addition was 20 min.

studies have shown that adsorption took place via the phosphate backbone (Liu & Liu 2014; Lopez *et al.* 2017). Moreover, C_6 had the highest adsorption and detachment affinity among four types of bases (Liu & Liu 2014; Lopez *et al.* 2017). We found that the fluorescence intensity increased as the As(V) concentration increased (Figure 4) due to the FAM- C_6 adsorbed onto CeO_2NPs was detached (Figure 1). The ΔF of the POS samples with C_{12} to C_{30} did not increase as the As(V) concentration increased due to C_{12} and longer ones adsorbed too tightly onto CeO_2NPs surfaces to detach. The FAM- C_6 could produce a higher sensitivity because it was easier to adsorb than the FAM- C_{12} and the longer ones. Previous studies showed that FAM- A_{15} was used for MnO_2NPs (Wang *et al.* 2018) and FAM- C_{15} were used for $\text{Fe}_3\text{O}_4\text{NPs}$ (Liu & Liu 2014) to achieve fluorescence quenching and recovering. We concluded that CeO_2NPs have the unique property to achieve higher sensitivity using shorter FAM-labeled DNA length.

Effect of the incubation time after adding samples on fluorescence intensity

Figure 5 shows the time course change in ΔF . The ΔF increased immediately within the initial 6 min, indicating that the detachment of FAM-labeled ssDNA from CeO_2NPs occurred within the initial 6 min. The ΔF maximum value at 18 min.

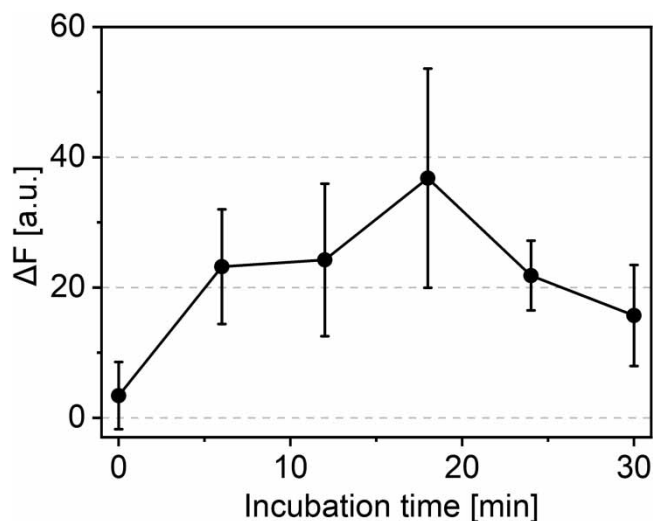


Figure 5 | Variation of ΔF of test solutions with time after sample addition in the POS and NEG. The final CeO_2NPs concentration was $15 \mu\text{g/mL}$, FAM- C_6 as FAM-labeled DNA was used and the final FAM- C_6 concentration was 400 nM .

In contrast, the ΔF did not increase until 18 min and increased thereafter. Based on these results, the optimal incubation time after sample addition was determined to be 6 min. The optimal incubation time was shorter than that in the previous studies using $\text{Fe}_3\text{O}_4\text{NPs}$ and MnO_2NPs (over 30 min) (Liu & Liu 2014; Wang *et al.* 2018). Such fast signaling kinetics is advantageous for analysis of As(V). This is likely because the density of FAM- C_6 on the CeO_2NPs surface was higher than $\text{Fe}_3\text{O}_4\text{NPs}$ and MnO_2NPs , which would accelerate the displacement reaction.

Calibration curve

Figure 6 shows a calibration curve of As(V) for the method. The ΔF of the test solutions remained unchanged below $0.5 \mu\text{M}$ As(V) and logarithmically increased from 40 to 200 with increase in As(V) concentrations from 0.5 to $2 \mu\text{M}$. The detection limit (LOD) was calculated to be $0.61 \mu\text{M}$. When the As(V) concentration exceeded $2 \mu\text{M}$, the ΔF increased further and remained almost unchanged at $50 \mu\text{M}$ As(III) (data not shown).

Method selectivity

Figure 7 shows the ΔF of the samples with different anions. The ΔF of the solution with As(V) was significantly higher than that of the blank sample. The ΔF of the samples with sulfate were slightly higher and the samples with carbonate and

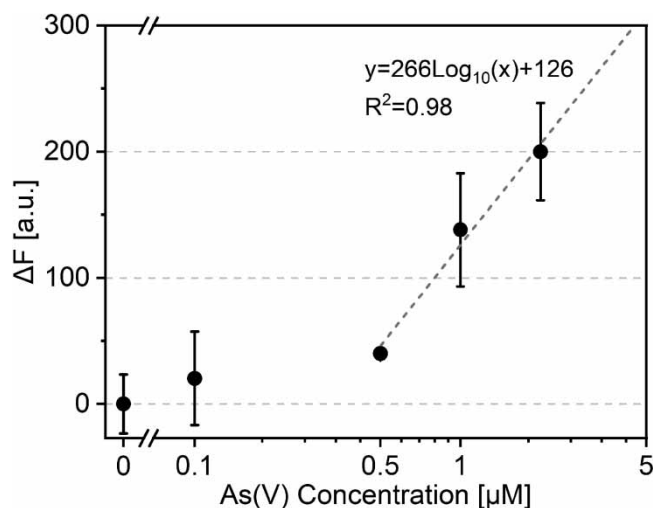


Figure 6 | Method calibration curve. The dotted line is a regression line.

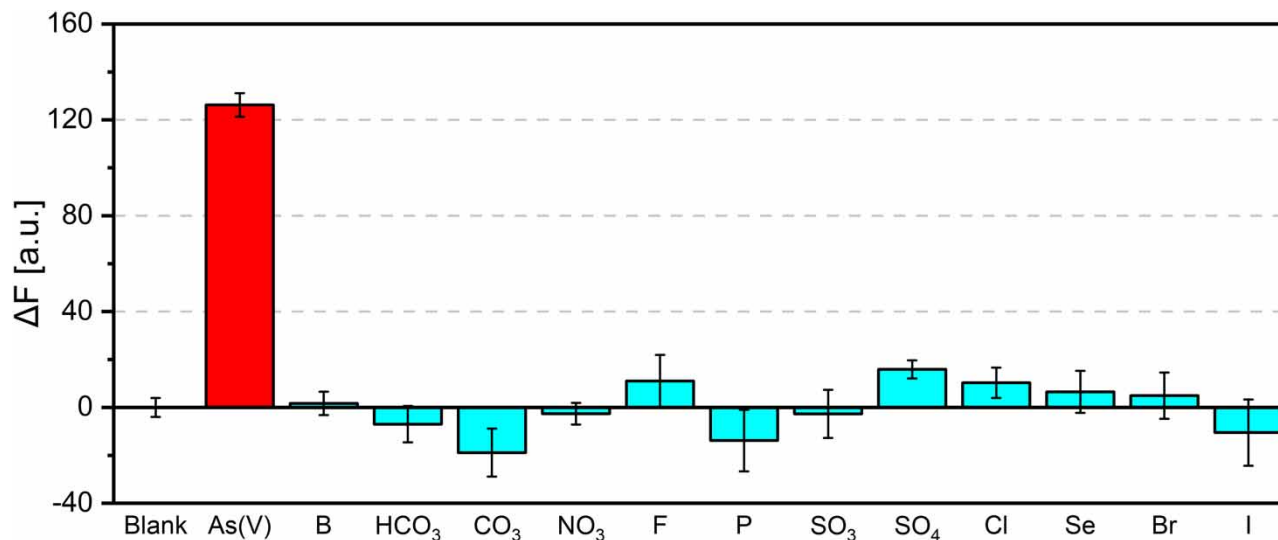


Figure 7 | Method selectivity for anions. The concentration of anion was 10 μ M.

phosphate were slightly lower than that of the blank sample. We conducted a statistical analysis among the anions. There were no statistically significant differences ($p > 0.05$) among blank and the other anions (except As(V)). However, when the inhibitory test was conducted using 100 μ M of the anions, borate and phosphate interfered with the method (Figure S2). When we made the calibration curve of the method using borate and phosphate instead of As(V), the fluorescence intensity increased with an increase in these anions (Figure S3). Therefore, we found that borate and phosphate were the main interfering substances in this method.

Figure 8 shows the ΔF of the samples with different cations. The ΔF of the solution with As(V) was significantly higher than that of the blank sample. There were no statistically significant differences ($p = 0.05$) in the ΔF of the samples with As(III), K(I), Ca(II), Mn(II), Fe(II), Fe(III), Co(II) and Ni(II) solutions against the blank sample. In contrast, ΔF values were slightly higher in the solutions of Na(I), Mg(II), Fe(III) and Zn(II) and significantly higher in the solutions with Cu(II), Cd(II), Hg(II) and Pb(II). However, we could remove these ions by pre-treatment applied in this study (see Figure S4). These results showed a high selectivity of the method toward As(V) after the pre-treatment.

Analysis of groundwater samples

Contrary to expectations, when GW without As(V) was subjected to the assay, the peak of fluorescence intensity at 518 nm increased significantly (Figure 9). The increase in the fluorescence band may be attributed to detachment of the FAM-C₆ by

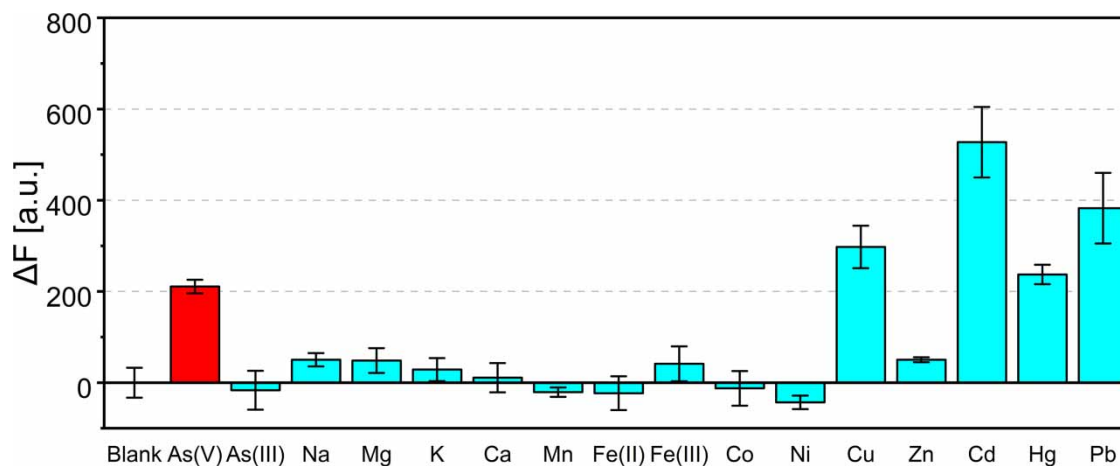


Figure 8 | Method selectivity for cations including As(V) and As(III). The concentration of each ion was 10 μ M.

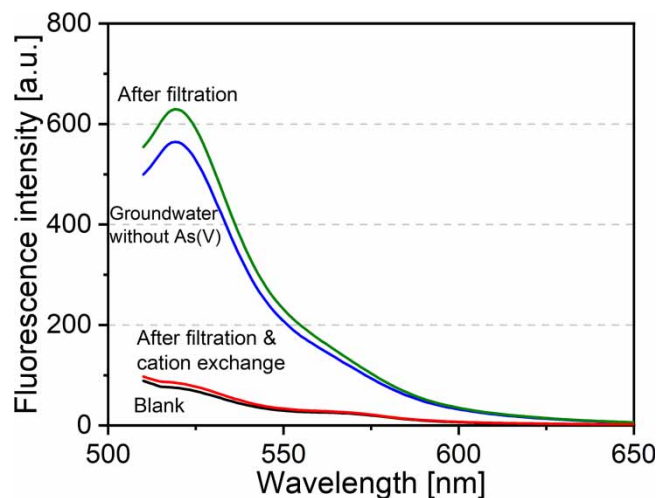


Figure 9 | Fluorescence intensity of FAM-labeled DNA in groundwater, groundwater filtered with 0.2- μm -pore-size membrane filter, and groundwater filtered with 0.2- μm -pore-size membrane filter and passed through cation-exchange resin.

the ions in the sample (Table S1). Therefore, the GW was pretreated with a 0.2- μm pore-size membrane filter and cation-exchange resin. Membrane filtration did not remove the interfering ions in the GW (Figure 9). In contrast, the peak of fluorescence intensity of the sample subjected to filtration followed by cation exchange was almost the same as that of a blank sample (Figure 9), indicating that the filtration followed by cation exchange could significantly reduce interfering effects of matrix of GW. Table S1 shows the ion concentrations in the GW before and after cation-exchange treatment. The GW contained divalent cations (i.e. Mg(II) and Ca(II)), which may explain the increase of the peak of fluorescence band (Figure S5). The results show that metal-cation concentrations in GW were efficiently removed by cation exchange and alternatively Na(I) was released.

Figure 10 shows the relationship between the concentrations of As(V) in GW determined by the method and HPLC-ICP-MS. Some plots show that As(V) concentrations determined by the method were almost identical to those by HPLC-ICP-MS. Our methods could determine As(V) concentration in groundwater between 0.1 and 1.0 μM . On the other hand, our methods could not determine As(V) concentration in groundwater above 2.5 μM because the standard deviations were larger and greatly overestimated (data not shown).

However, As(V) concentrations of most of the samples have the large measurement error because Na(I) was the sole ion present in the pre-treatment samples (Table S1) and standard error of the results was large. Therefore, we need to modify the method to reduce the measurement error.

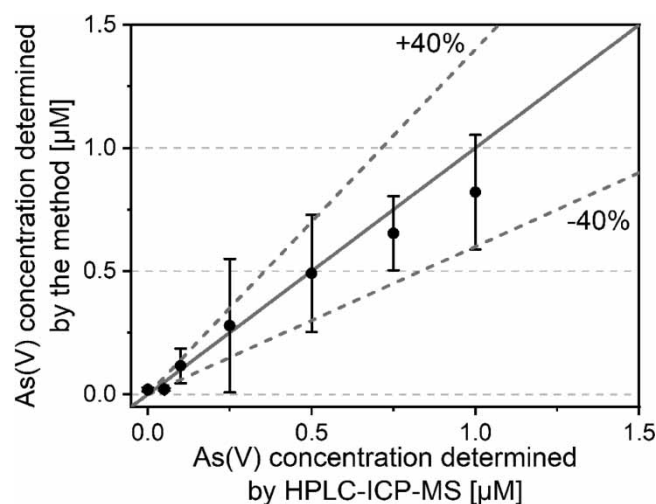


Figure 10 | Relationship between concentrations of As(V) determined by HPLC-ICP-MS and those determined by using the method.

Lakatos *et al.* (2015) developed a simple analytical method for As(V) using S-layer functionalized gold nanoparticles (Lakatos *et al.* 2015). Das & Sarkar (2016) developed the As(V) sensor based on antimonyl–arseno–molybdate complex in the presence of ammonium molybdate, potassium antimonyl tartrate and ascorbic acid. However, As(III) is also adsorbed onto gold nanoparticles (Zong & Liu 2019) and the selectivity between As(III) and As(V) is not shown in the study (Lakatos *et al.* 2015). The As(V) sensor that Das & Sarkar (2016) developed can measure As(V) concentration by color shading, which is not suitable for low concentration As(V) analysis because the LOD is higher than that of our method.

The merit of our method is that it is selective for As(III). It is because the simple analytical methods for As have been developed only for As(III) and total As, but not for As(V). On the other hand, the disadvantage of our method is that it is subject to interference by other anions such as borate and phosphate at high concentrations. Since there is no simple technique to separate As(V) from borate and phosphate, our method cannot be applied to samples with high concentrations of borate and phosphate.

Determining various chemical species such as As(III) and As(V) is a quite challenging task. The instrumental methods, such as LC-ICP-MS, are not common to determine the concentration of various As species. In this regard, developing the methods for analysis of various As species is of importance. Our method relies on the strong interaction between As(V) and the surface of metal oxide nanoparticles and provides an inexpensive, simple, and easy-to-use platform.

CONCLUSION

In this study we developed a simple analytical method to determine As(V) concentrations using CeO₂NPs and a FAM-labeled ssDNA and firstly attempted to measure the concentration of As(V) in groundwater by the method. The parameters that affect the method performance, such as the final concentration of CeO₂NPs (15 µg/mL) and FAM-labeled DNA (400 nM), the sequence and length of FAM-labeled DNA (FAM-C₆) and incubation time (6 min) with samples were optimized. After optimizing the parameters, the total analysis time was about 20 min and the LOD was 0.61 µM. This method has a significant selectivity against the same concentrations of Cu(II), Cd(II), Hg(II) and Pb(II) and a slight selectivity against the same concentrations of sulfate and carbonate. For cations, pre-treatment by cation extraction to remove interfering ions was beneficial for determination of As(V) concentrations in groundwater containing a variety of metal cations at high concentration. We could underestimate the As(V) concentrations in As(V)-spiked GW by the method. In the future, we should reduce the standard deviation and stabilize the adsorption and detachment of FAM-labeled DNA and As(V) onto CeO₂NPs. This method has potential in the development of an As(V) sensor for application to on-site analysis.

ACKNOWLEDGEMENTS

This research was supported financially by JSPS KAKENHI [grant number 21H04568, 20KK0090, 17H03328, 26289178, 23686074], and the Matching Planner Program from Japan Science and Technology Agency [grant number JPMJTM15KU]. We thank Prof. Ayumi ITO and Ms Yumi Kawamura for As measurements by HPLC-ICP-MS.

DATA AVAILABILITY STATEMENT

All relevant data are included in the paper or its Supplementary Information.

REFERENCES

- Amini, M., Abbaspour, K. C., Berg, M., Winkel, L., Hug, S. J., Hoehn, E., Yang, H. & Johnson, C. A. 2008 *Statistical modeling of global geogenic arsenic contamination in groundwater*. *Environmental Science & Technology* **42** (10), 3669–3675. <http://dx.doi.org/10.1021/es702859e>.
- Baghbaderani, S. S. & Noorbakhsh, A. 2019 *Novel chitosan-Nafion composite for fabrication of highly sensitive impedimetric and colorimetric As(III) aptasensor*. *Biosensors and Bioelectronics* **131** (February), 1–8. <https://doi.org/10.1016/j.bios.2019.01.059>.
- Bülbül, G., Hayat, A., Mustafa, F. & Andreescu, S. 2018 *DNA assay based on Nanoceria as Fluorescence Quenchers (NanoCeracQ DNA assay)*. *Scientific Reports* **8** (1), 2426. <http://www.nature.com/articles/s41598-018-20659-9>.
- Chowdhury, U. K., Biswas, B. K., Chowdhury, T. R., Samanta, G., Mandal, B. K., Basu, G. C., Chanda, C. R., Lodh, D., Saha, K. C., Mukherjee, S. K., Roy, S., Kabir, S., Quamruzzaman, Q. & Chakraborti, D. 2000 *Groundwater arsenic contamination in Bangladesh and West Bengal, India*. *Environmental Health Perspectives* **108** (5), 393–397.
- Chung, C. J., Huang, Y. L., Huang, Y. K., Wu, M. M., Chen, S. Y., Hsueh, Y. M. & Chen, C. J. 2013 *Urinary arsenic profiles and the risks of cancer mortality: a population-based 20-year follow-up study in arseniasis-endemic areas in Taiwan*. *Environmental Research* **122**, 25–30. <http://dx.doi.org/10.1016/j.envres.2012.11.007>.

- Clancy, T. M., Hayes, K. F. & Raskin, L. 2013 Arsenic waste management: a critical review of testing and disposal of arsenic-bearing solid wastes generated during arsenic removal from drinking water. *Environmental Science and Technology* **47** (19), 10799–10812.
- Das, J. & Sarkar, P. 2016 A new dipstick colorimetric sensor for detection of arsenate in drinking water. *Environmental Science: Water Research & Technology* **2** (4), 693–704. <http://xlink.rsc.org/?DOI=C5EW00276A>.
- Flora, S. J. S. 2015 *Handbook of Arsenic Toxicology*. Academic Press, London.
- Hafuka, A., Nagasato, T. & Yamamura, H. 2019 Application of graphene oxide for adsorption removal of geosmin and 2-Methylisoborneol in the presence of natural organic matter. *International Journal of Environmental Research and Public Health* **16** (11), 1–8.
- Kamei-Ishikawa, N., Segawa, N., Yamazaki, D., Ito, A. & Umita, T. 2017 Arsenic removal from arsenic-contaminated water by biological arsenite oxidation and chemical ferrous iron oxidation using a down-flow hanging sponge reactor. *Water Science and Technology: Water Supply* **17** (5), 1249–1259.
- Kaur, H., Kumar, R., Babu, J. N. & Mittal, S. 2015 Advances in arsenic biosensor development – a comprehensive review. *Biosensors and Bioelectronics* **63**, 533–545. <http://dx.doi.org/10.1016/j.bios.2014.08.003>.
- Lakatos, M., Matys, S., Raff, J. & Pompe, W. 2015 Colorimetric As (V) detection based on S-layer functionalized gold nanoparticles. *Talanta* **144**, 241–246. <http://dx.doi.org/10.1016/j.talanta.2015.05.082>.
- Liu, B. & Liu, J. 2014 DNA adsorption by magnetic iron oxide nanoparticles and its application for arsenate detection. *Chemical Communications* **50** (62), 8568. <http://xlink.rsc.org/?DOI=C4CC03264>.
- Liu, B. & Liu, J. 2015 Comprehensive screen of metal oxide nanoparticles for DNA adsorption, fluorescence quenching, and anion discrimination. *ACS Applied Materials and Interfaces* **7** (44), 24833–24838.
- Lopez, A., Zhang, Y. & Liu, J. 2017 Tuning DNA adsorption affinity and density on metal oxide and phosphate for improved arsenate detection. *Journal of Colloid and Interface Science* **493**, 249–256. <http://dx.doi.org/10.1016/j.jcis.2017.01.037>.
- Matsunaga, K., Okuyama, Y., Hirano, R., Okabe, S., Takahashi, M. & Satoh, H. 2019 Development of a simple analytical method to determine arsenite using a DNA aptamer and gold nanoparticles. *Chemosphere* **224**, 538–543. <https://linkinghub.elsevier.com/retrieve/pii/S0045653519304060>.
- Muppudathi, M., Perumal, P., Ayyanu, R. & Subramanian, S. 2019 Immobilization of ssDNA on a metal-organic framework derived magnetic porous carbon (MPC) composite as a fluorescent sensing platform for the detection of arsenate ions. *The Analyst* **144** (9), 3111–3118.
- Pautler, R., Kelly, E. Y., Huang, P. J. J., Cao, J., Liu, B. & Liu, J. 2013 Attaching DNA to nanoceria: regulating oxidase activity and fluorescence quenching. *ACS Applied Materials and Interfaces* **5** (15), 6820–6825.
- Pena-Pereira, F., Villar-Blanco, L., Lavilla, I. & Bendicho, C. 2018 Test for arsenic speciation in waters based on a paper-based analytical device with scanometric detection. *Analytica Chimica Acta* **1011**, 1–10. <https://doi.org/10.1016/j.aca.2018.01.007>.
- Singh, R., Singh, S., Parihar, P., Singh, V. P. & Prasad, S. M. 2015 Arsenic contamination, consequences and remediation techniques: a review. *Ecotoxicology and Environmental Safety* **112**, 247–270. <http://dx.doi.org/10.1016/j.ecoenv.2014.10.009>.
- USEPA 2018 *National Primary Drinking Water Regulations*. Available from: <https://www.epa.gov/ground-water-and-drinking-water/national-primary-drinking-water-regulations>.
- Wang, L., Huang, Z., Liu, Y., Wu, J. & Liu, J. 2018 Fluorescent DNA probing nanoscale MnO₂: adsorption, dissolution by thiol, and nanozyme activity. *Langmuir* **34** (9), 3094–3101.
- WHO 2011 *Guidelines for Drinking-Water Quality*, 4th edn. Available from: <http://scholar.google.com/scholar?hl=en&btnG=Search&q=intitle:Health+Criteria+and+Other+Supporting+Information#1%5Cnhttp://scholar.google.com/scholar?hl=en&btnG=Search&q=intitle:Health+criteria+and+other+supporting+information%231>.
- Wu, Y., Liu, L., Zhan, S., Wang, F. & Zhou, P. 2012a Ultrasensitive aptamer biosensor for arsenic(iii) detection in aqueous solution based on surfactant-induced aggregation of gold nanoparticles. *The Analyst* **137** (18), 4171–4178. <http://dx.doi.org/10.1039/C2AN35711A>.
- Wu, Y., Liu, L., Zhan, S., Wang, F. & Zhou, P. 2012b Ultrasensitive aptamer biosensor for arsenic(iii) detection in aqueous solution based on surfactant-induced aggregation of gold nanoparticles. *The Analyst* **137** (18), 4171–4178. <http://xlink.rsc.org/?DOI=c2an35711a>.
- Xu, X., Wang, L., Zou, X., Wu, S., Pan, J., Li, X. & Niu, X. 2019 Highly sensitive colorimetric detection of arsenite based on reassembly-induced oxidase-mimicking activity inhibition of dithiothreitol-capped Pd nanozyme. *Sensors and Actuators B: Chemical* **298** (July), 126876. <https://doi.org/10.1016/j.snb.2019.126876>.
- Zhan, S., Yu, C. M. & Lv, C. J. 2014 Colorimetric detection of trace arsenic (III) in aqueous solution using arsenic aptamer and gold nanoparticles. *Australian Journal of Chemistry* **67**, 813–818.
- Zong, C. & Liu, J. 2019 The arsenic-binding aptamer cannot bind arsenic: critical evaluation of aptamer selection and binding. *Analytical Chemistry* **91**, 10887–10893.

First received 11 October 2021; accepted in revised form 12 March 2022. Available online 24 March 2022